Indonesian Physical Review
Volume 08 Issue 02, May 2025
P-ISSN: 2615-1278, E-ISSN: 2614-7904

A Non-Linear Hypocenter Localization along the Active Palu-Koro Fault: A Case Study Central Sulawesi

Harsano Jayadi[1*], Moh. Dahlan Th. Musa[1], Gazali Rachman[2], Icha Untari Meidji[3], Muhammad Fawzy Ismullah Massinai[4], Dwa Desa Warnana[5]
[1] *Geophysical Engineering Study Program, University of Tadulako, Indonesia*
[2] *Physics Education-FKIP, Pattimura University of Ambon-Molucca, Indonesia*
[3] *Department of Physics, Universitas Negeri Gorontalo, Indonesia*
[4] *Department of Geophysics, Universitas Hasanuddin, Indonesia*
[5] *Department of Geophysical Engineering, Institut Teknologi Sepuluh Nopember, Indonesia*

Corresponding Authors E-mail: harsanoj@gmail.com

Article Info

Article info:
Received: 19-10-2024
Revised: 02-03-2025
Accepted: 17-03-2025

Keywords:
Earthquake Location; Palu-Koro Fault; Seismicity Zone; Central Sulawesi

How To Cite:
H. Jayadi, M. D. Th. Musa, G. Rachman, I. U. Meidji, M. F. I. Massinai, and D. D. Warnana, "A Non-Linear Hypocenter Localization along the Active Palu-Koro Fault: A Case Study Central Sulawesi", Indonesian Physical Review, vol. 8, no. 2, p 400-416, 2025.

DOI:
https://doi.org/10.29303/ipr.v8i2.418.

Abstract

The Central Sulawesi region is prone to earthquakes, as evidenced by its complex geological structure. Several plates and active fault movements in the vicinity cause this situation. One of the active faults that often causes earthquakes is the Palu-Koro active fault. The city of Palu is one of the areas passing through the Palu-Koro fault. The danger of this earthquake occurrence can be ascertained and assessed using a suitable earthquake location. Within the scope of our investigation, we used a non-linear approach to predict the hypocenter site in the vicinity of the Palu-Koro fault that is active. This Method use oct-tree importance sampling algorithm to generate spatial hypocenter locations. Using the AK135 minimal seismic velocity model, we manually re-picked the arrival times of wave P-waves and S-waves arrival timings of 3,852 and 3,690, respectively, collected by 24 BMKG observation sites from January 2011 to December 2015, utilizing the minimal 1D seismic velocity model from AK135. We employed criteria to ascertain the event's location, including a minimum of four stations exhibiting a distinct beginning of P and S wave arrivals, with a magnitude of at least 3Mw and an average depth ranging from 10 to 20 km. The outcomes of seismic event location identification exhibit improved clustering with inversion, revealing a zero-centered Gaussian distribution, where more time discrepancies, both positive and negative, correspond to increased estimating mistakes. According to this research, the Palu-Koro active fault line's primary shallow seismic zone is the most prominent feature in the area and confirms the existence of active land faults that cause earthquake events by conducting a process of determining a locally updated 1D velocity model that will be used to determine a more precise relocation of the hypocenter used to interpret the subsurface model of the research area.

Introduction

As a large country, Indonesia is also one of the most populated areas due to its location on three major oceans: the Pacific, which is located on the east coast of the Pacific, the Eurasia on the west coast of the Pacific, and the Indo-Australian on the east coast of Australia [1], [2]. Sulawesi Island is a landlocked island in the eastern part of Indonesia, influenced by the tectonics of Eurasia in the south, the micro-Filipina in the north, the Pacific in the south, and the Indo-Australian in the south. This also contributes to Sulawesi's stratigraphic position changing, as shown in Figure 1.

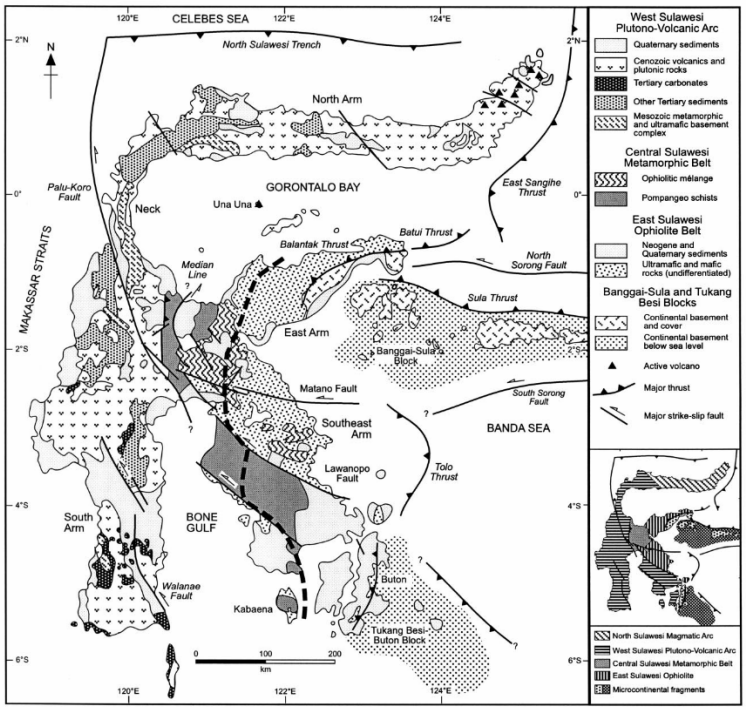

Figure 1. The geological road map of Sulawesi Island shows the geological configuration and location of the Palu Koro fault in a black solid line [3]

The underlying tectonic processes, faults, troughs, thrusts and spread centres in Sulawesi Island seismic activity is frequently impacted by events in Bone Bay and the Makassar Strait. [4], [5]. The activity encompasses the Palu Koro, Walanae, Matano, Hamilton, and Sorong (south Sula-Sorong) faults, as well as subduction troughs represented by North Sulawesi, Sangihe, Tolo, and the Batui and Sula trusts. The Palu Koro fault, the Sulawesi trough, and the Sangihe trough are the predominant tectonic causes contributing to disaster development in the Sulawesi region [6], [7].

Sulawesi is a region situated at the convergence of the Eurasian, Indo-Australian, Pacific, Philippine Sea, and Sundaland tectonic plates [8]. Furthermore, Sulawesi is influenced by microcontinents including the Molucca Sea, Banda Sea, Timor, Birds Head, and Caroline [9]. This signifies an intricate tectonic environment marked by seismic activity. Sulawesi is distinguished by seismic and volcanic activity. Earthquakes with epicentres on central Sulawesi are closely associated with the activity of the Palu Koro Fault.

Palu Koro is an active strike-slip fault situated among three tectonic plates: the Eurasian plate, the Pacific plate, and the Indo-Australian plate, along with the Philippine microplate. This

configuration renders it a significant source of high seismicity on the island of Sulawesi, particularly in the Central Sulawesi region [11], [12]. This fault delineates the Makassar block from the northern block of Sula [13], exhibiting a relative displacement of approximately 40 mm/yr across Palu Bay towards northern Palu and western Minahasa until it intersects the North Sulawesi subduction zone [10], [12], [14], [15].

Accordingly, based on several studies conducted in the Sulawesi region, especially in the Palu Koro fault zone, it is evident that this fault exhibits significant activity characterized by escalating seismic occurrences [10], [12] and has historically triggered tsunami events in 1927, 1938, 1967, 1968, 1969, 1996, and 2018 [10], [16], [17], [18]. In the Sulawesi region, particularly in the structurally unstable Palu Koro fault zone, more comprehensive research is urgently needed to investigate the subsurface structural models that can lead to develop measures for disaster mitigation and to do additional research on the Palu-Koro Fault and other faults located in the central region of Sulawesi.

Numerous studies have been undertaken in Central Sulawesi, particularly to observe the evolution of the active Palu-Koro fault, employing seismological [19], [20], geodetic [21], and geological [22] methodologies. These studies indicate that seismicity and deformation levels are significantly high. The focal mechanism identified in the Palu Koro fault zone is a normal shear fault, exhibiting a coseismic stress Coulomb model characterized by multiple ruptures and both positive and negative overlays along the Palu Bay coastline.

Analysis of the conditions in several studies confirms that the region surrounding the active Palu-Koro fault exhibits considerable seismicity, therefore underscoring the necessity of investigating its structure and tectonic dynamics. Consequently, an alternative approach is required to ascertain the hypocenter of earthquakes in the vicinity of the Palu-Koro fault. Estimating a more precise and reliable hypocenter location for seismic data analysis is beneficial in addressing the ambiguity and complexity inherent in earthquake data processing. This study employs the non-linear technique established by Lomax [23]. The non-linear approach we used in this study is to overcome or add to the limitations that exist in the linear/conventional method, especially in determining heterogeneous wave velocity variations below the earth's surface. On the other hand, this non-linear method is also better in determining hypocentres using data whose signals are affected by noise. This is because the non-linear method uses a more accurate evaluation of data uncertainty and statistical approaches [24]. The identical methodology has been utilized in Western Java [25], Eastern Java [26], and the Molucca Sea region [27], when attempting to determine earthquake hypocenters, the catalogue data provided by the Meteorological, Climate and Geophysical Agency (BMKG) yielded positive findings.

Regional Geology

Seismotectonic research indicates that the island of Sulawesi is unstable due to the collisional interactions among the Pacific, Asian, and Australian plates [10]. Sulawesi Island comprises an outer arc belt and an inner arc belt, both of which experience variations characterized by low temperatures and high pressures, as well as high temperatures and low pressures, believed to be associated with subduction and corresponding volcanic arcs [3], [28]. The Sulawesi Island region, situated at the convergence of multiple tectonic plates, specifically the Pacific, Eurasian, Indo-Australian, Philippine Sea, and Sundaland plates, is susceptible to

seismic and volcanic activity due to various large and small-scale faults, including the active Palu Koro fault [5], [29].

Numerous fault segmentations frequently induce significant earthquakes in the Sulawesi region, particularly in Central and South Sulawesi [30], including the Palu Koro fault, Saddang fault, and associated trenches, which feature various geological characteristics such as folds and fractures. Vertical fissures are present in the northern region. In contrast, the western section exhibits horizontal displacement to the left [31], with a projected movement velocity of 14-17 mm/year [32].

The Palu Koro fault, predominantly situated in Central Sulawesi, is an exceptionally active fault contributing to a significant degree of vulnerability in the region. This is intrinsically linked to its position at the convergence of the Eurasian, Pacific, and Indo-Australian tectonic plates, which are engaged in ongoing convergent and collisional movements [33]. Seismicity data from the Palu Koro fault zone show high earthquake activity, with earthquakes primarily occurring at depths ranging from 0 to 60 km, which corresponds to the energy released by the Palu Koro fault's movement. The seismicity distribution in the Sulawesi Island region has been mapped [35], [36], demonstrating that the northern section of Sulawesi experiences earthquakes at deeper depths, primarily in maritime areas; yet the Sulawesi tectonic map suggests that there are no faults in this region [37]. As Figure 2 shows.

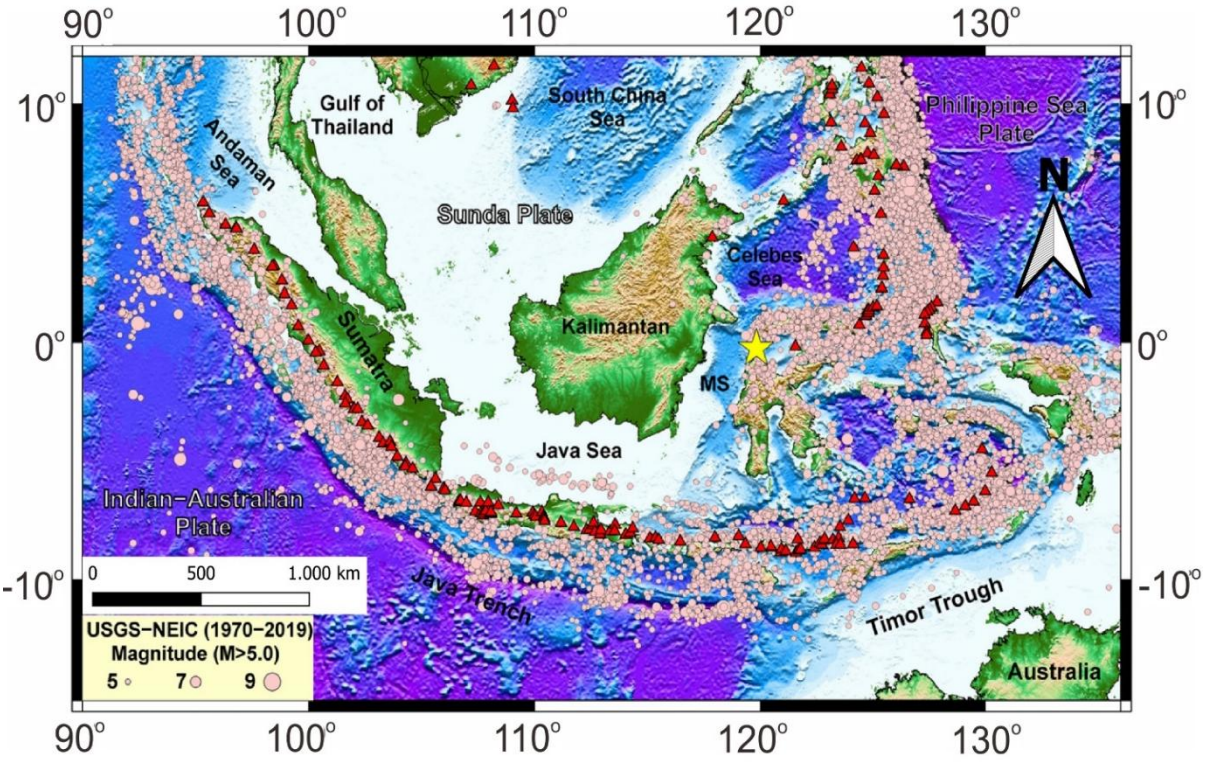

Figure 2. Examination of seismic activity in the Sulawesi region (Indonesia) involving earthquakes with magnitudes of 5 M or above. The 7.5 Mw earthquake of 2018 in Palu (Sulawesi) is indicated by a yellow star. The red triangles represent volcanoes located across Indonesia. The data was obtained from the USGS-NIEC earthquake database covering the years 1970 to 2017 [35].

The intricate geodynamic processes in the Sulawesi region induced alterations that fractured all rock types, culminating in a very complicated stratigraphic model characterized by the invasion of granite rock domes and the development of new fractured structures, shear failures and normal failures. The Palu Koro fault line is presently identifiable as a surface rupture trace that curves in Palu Bay (West-East) toward the western neck of Sulawesi [34]. Conversely, fault movement can induce a nearby rock to have a significantly elevated permeability value, resulting in more energy generation, which can lead to an increase in the thermal properties of the surrounding rock. Consequently, elevated rock permeability combined with high temperature will lead to the accumulation of geothermal energy.

Theory and Calculation

The preliminary phase of the analysis of earthquake data includes identifying hypocentres and determining the location and depth of the earthquake by re-assessing the arrival times of the P-waves and S-waves. This study employs a non-linear locating method utilizing software to ascertain the hypocentre of an earthquake. This study employs the non-linear localization method utilizing NonLinLoc software [23]. The NLLoc program generates a misfit function that identifies the 'ideal' hypocenter by determining the probability density function (PDF). Utilize a Probability Density Function (PDF) to ascertain the coordinates of the x, y, and z hypocentres employing one of the following methods: grid search systematic, stochastic metropolis-gibbs, or oct-tree significance sampling techniques.

The algorithm employed in locating earthquakes within the NLLoc software incorporates the methodologies of [35] and [36], alongside the inversion technique proposed by [36]. Inaccuracies in the observation of the re-selected arrival time and the calculation of the journey time are assumed to follow the Gaussian distribution. This assumption facilitates a direct analytical computation of the most significant likelihood origin time, derived from the observation arrival time and the journey time calculation between the station and each point in XYZ space. The inversion formula employed in the NLLoc program relies on utilizing normalized on unnormalized probability density functions to f(x) determine the parameter values. The probability measurements of x in intervals (X,X+ΔX) are obtained by normalization of the density function f(x) of the x variable.

$$P(X \leq x \leq X + \Delta X) = \int_X^{X+\Delta X} f(x)dx \quad (1)$$

In ascertaining earthquake sites, the unknown variables encompass the hypocentral coordinates x=(x,y,z) and the origin time T. The observational data includes the arrival time t, whereas the theoretical model offers the anticipated trip time h. Considering that the theoretical relationship and the observed arrival time exhibit Gaussian uncertainties characterised by covariance matrices C_T and Ct, and presuming uniform prior information at T, one can analytically compute the integral over d in Equation (2) and the integral over the origin time T to derive the marginal probability density function for the spatial locations (x).

$$\sigma_P(P) = \rho_p(\boldsymbol{P}) \int \frac{\rho_{d(\boldsymbol{d})}\theta(\boldsymbol{d}|\boldsymbol{p})}{\mu_d(\boldsymbol{d})} d\boldsymbol{d} \quad (2)$$

In an inversion, it is essential to restrict the values of a vector of unknown parameters p by utilising a vector of observable data d, which theoretically relates as $\theta(d,p)$. The density function offers initial insights into the model parameters $\rho_p(\mathbf{p})$ and the independent observations ρd($\mathbf{d}$), which can be articulated as a conditional density function. $\theta(d \mid p)$ $\mu_p(\mathbf{p})$ is a comprehensive probabilistic solution articulated as a Posterior Density Function (PDF) $\sigma_p(\mathbf{p})$, where in $\mu_p(\mathbf{p})$ and $\mu_d(\mathbf{d})$ serve as the foundational information density functions reflecting a state of complete ignorance [25], [40].

An oct-tree importance sampling approach is employed to enhance the precision of event site determination, proving efficient and thorough for earthquake probability density function localization in three-dimensional space (x, y, z). This method is straightforward, requiring just a limited number of parameters, and is significantly faster and more stable than the Metropolis-Gibbs method, being 100 times quicker than Grid Search [37]. This method involves an initial global sample of the misfit function on a coarse grid, succeeded by iterative implementation as detailed below: Partition the grid cell exhibiting the highest location probability P (where P = PDF * cell volume) into eight subcells ($2x$, $2y$, $2z$), and evaluate the misfit function within each of the eight subcells, as depicted in Figure 3.

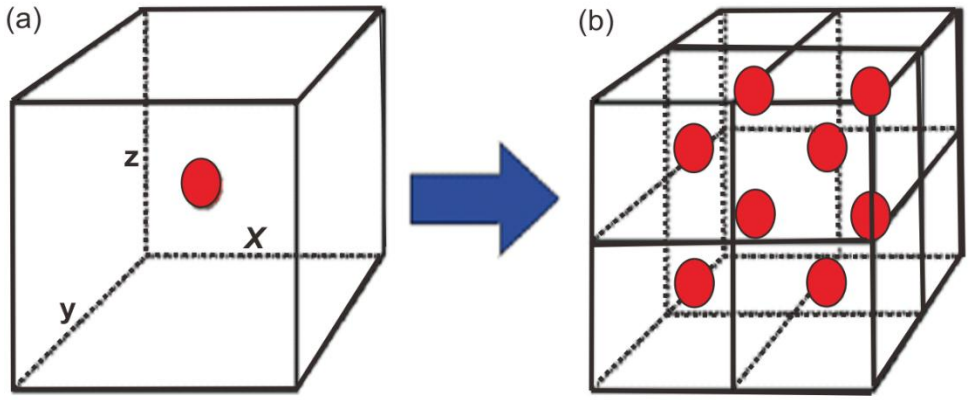

Figure 3. Depiction of sample volume with the octree approach. The red dots represent sample cell volumes. (a) one sample of the cell volume, (b) Eight new samples of the cell volume divided by eight.

A three-dimensional sample cell is recursively partitioned into eight segments. This results in a swift convergence into a series of overlapping arrays constituting an oct-tree structure of probability density function (PDF) value locations in three-dimensional space. The density of the sample cell is ascertained by the PDF value at the cell's center, emphasizing large PDF values to reduce discrepancies. Simultaneously, the likelihood of an earthquake occurring in the i-th cell can be determined using the subsequent equation.

$$P_i = V_i \, PDF \, (X_i) \tag{3}$$

where Vi represents the cell volume and Xi denotes the coordinates of the central cell.

The essence of the approach is a sequential array (Lp) of probability values Pi for all prior samples, ranging from the maximum PDF value P_{max} to the minimum PDF value P_{min}. The oct-tree sampling method commences with a global sampling of the whole search space, approximately arranged in a regular grid. The misfit value $g_i(x)$ in the center of each grid cell is ascertained, the probability Pi is computed, and the cell is incorporated into the probability list (Lp) at the position corresponding to its probability Pi.

Experimental Method

The study used waveform data from the Meteorological, Climate and Geophysical Agency (BMKG) available online (http://geof.bmkg.go.id/webdc3/) covering the period from 1 January 2011 to 31 December 2015, which were very close to the active Palu-Koro fault zone. The data were collected from 24 BMKG networks distributed in the entire area of study and are 3 magnitude as shown in Figure 5. During this period, a total of 378 earthquakes occurred near the active fault area of Palu-Koro. For each event, a re-choice was carried out to obtain the P-phase and the S-phase as inputs for the hypocenter location.

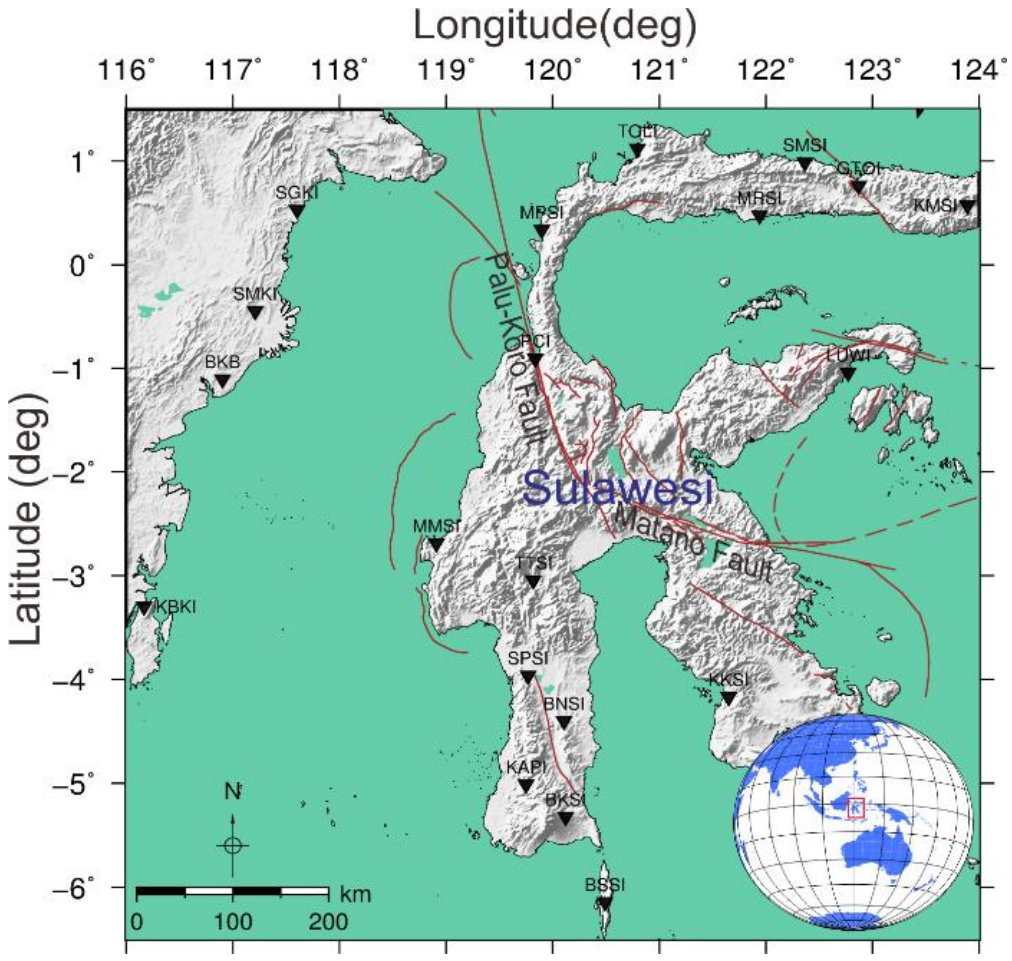

Figure 5. Geographical distribution of BMKG network monitoring stations that document seismic activity within the research region. The recording stations are represented by black inverted triangles.

Data re-picking was conducted utilizing the SeisGram2K70 v7.0 tool on seismic data files with the. mseed extension. The re-picking process was performed individually for 378 seismic data events. In an ideal scenario, each event would be documented by all 24 observing stations; however, in practice, data is only obtained from select stations for each event, where both P and S phase waveforms can be distinctly identified. This constraint stems from multiple difficulties, including station distance, noise, subsurface conditions, and other reasons that impede accurate sensor recording.

Each station was documented utilizing three components: vertical component (BHZ), east-west component (BHE), and north-south component (BHN). The re-picking of the P-wave arrival time relies on the BHZ component, whereas the re-picking of the S-wave arrival time depends on the BHE or BHN component. Upon re-picking, both the P-phases and S-phases will document and retain the station name, re-picked component, phase designation (P or S), date (day-month-year), arrival time, and gaussian (Figure 6).

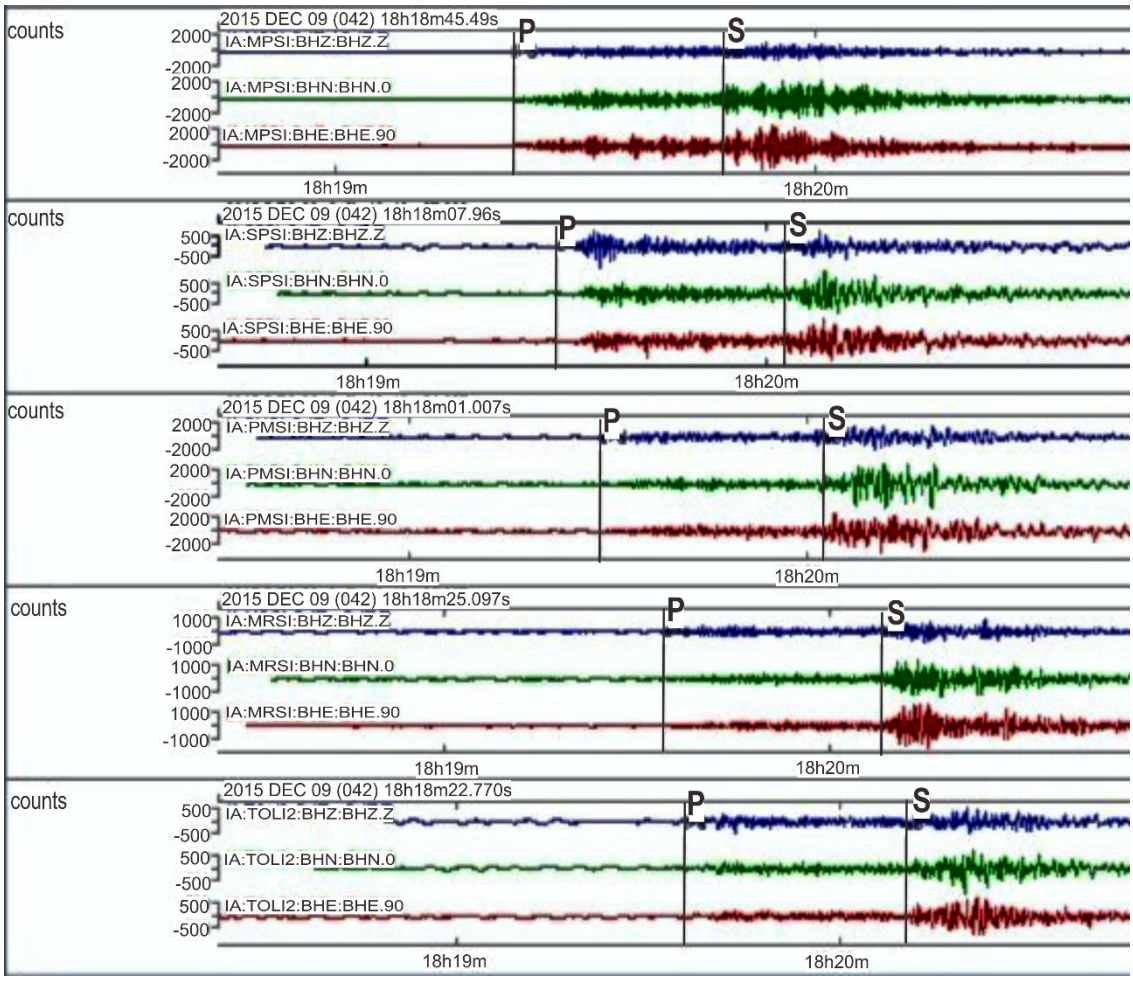

Figure 6. The process of re-picking arrival times for the P and S wave phases was based on the BHE, BHN and BHZ components of the observing stations that recorded earthquake events around the study area.

To identify erroneous re-picks or outliers in the P-phases and S-phases, a Wadati diagram is constructed, which juxtaposes the outcomes of the present re-pick with those of the previous re-pick. The Wadati diagram is created by comparing the re-pick results from a certain station with those from other stations linked to the same event. Re-evaluate outcomes from alternative stations within the same event. This supports the correctness of the re-pick phase results; the more linear the data, the more dependable it is. The greater the data's linearity, the higher its reliability. In the Wadati diagram, the arrival time of each P phase (horizontal axis Tp) and the difference between the arrival times S-P (vertical axis Ts-Tp) yield a straight trendline at the crossing point, as illustrated in Figure 7.

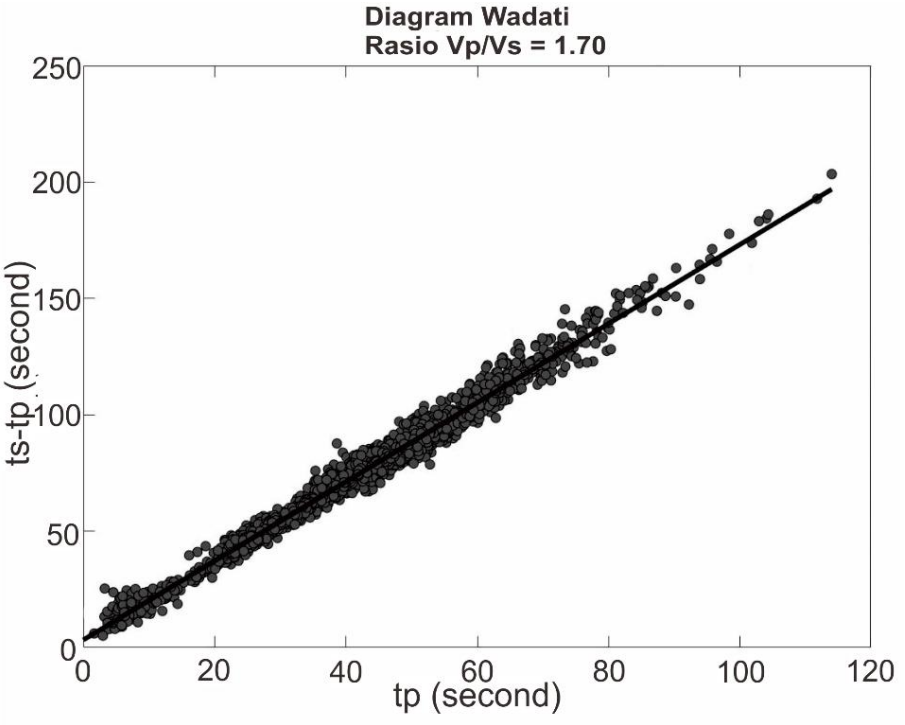

Figure 7. The Wadati diagram illustrates the arrival times of re-pick results for P-phases and S-phases to identify data outliers.

The Wadati diagrams are essential in delineating the arrival times of P-waves and S-waves; any point deviating from the linear trend may indicate a poorly diagnosed phase, potentially resulting from inaccuracies in phase identification. The phase needs to be better defined due to re-pick mistakes or inaccurate wave phase measurements, particularly for the arrival time. Re-selection or inaccurate interpretation of the wave phase, particularly the arrival timing of the S-waves or the morphology of the waveform after the P-waves. After the P-waves, the S-waves exhibit a very uniform shape, complicating the detection of subsequent waveform alterations. They are challenging to identify other waveform alterations. If numerous data points between P and S-P exhibit poor fitting, the data falls into the inadequate category [38].

The Non-Linear Location method for determining hypocenter locations is implemented in the NonLinLoc application, a suite of programs designed for constructing seismic velocity models, calculating travel times and probabilities, tracing global earthquake locations within 3-D structures, and visualizing 3-D data volumes. In this investigation, NonLinLoc Global mode-spherical coordinates were employed, taking into account the distribution of events and stations [23].

The approach uses a probabilistic inversion method and algoritm developed by Tarantola and Valet [40]. Furthermore, we used a sampling procedure of the significance of the oct tree to estimate the posterior density function (PDF) of the spatial center point [42]. This method offers a resolution to the challenge of converging and detecting volumetric anomalies, an enhanced probability density function, and minimal residual values. This strategy has been effectively established by [39] in Yellowstone and by [40] in Southwest Iberia. To obtain the probability density function of the three-dimensional hypocenter position, the oct tree

approach divides the most likely sampled cells into eight subordinate cells. This allows the calculation method of probability density functions. After fulfilling the end-of-the-year requirements, the procedure continues to be iterative. In order to identify the effects, we used the AK135's minimal one-dimensional seismic velocity model [43].

Results and Discussion

Our re-picking method accurately identified the P-waves and S-waves phases of 378 seismic events. The count of wave phases is 3852 for the P-phases and 3690 for the S-phases. The documented wave arrival times were depicted in a dyadic figure (Figure 8) to independently confirm the linear correlation between the P-phases and S-phases. The dyadic diagram analysis yielded a line slope 0.70, resulting in a Vp/Vs ratio 1.70. The measured locations or arrival times of the P-waves and S-waves exhibit a linear connection, and the timing accuracy of each phase is sufficient to determine the hypocenter's location.

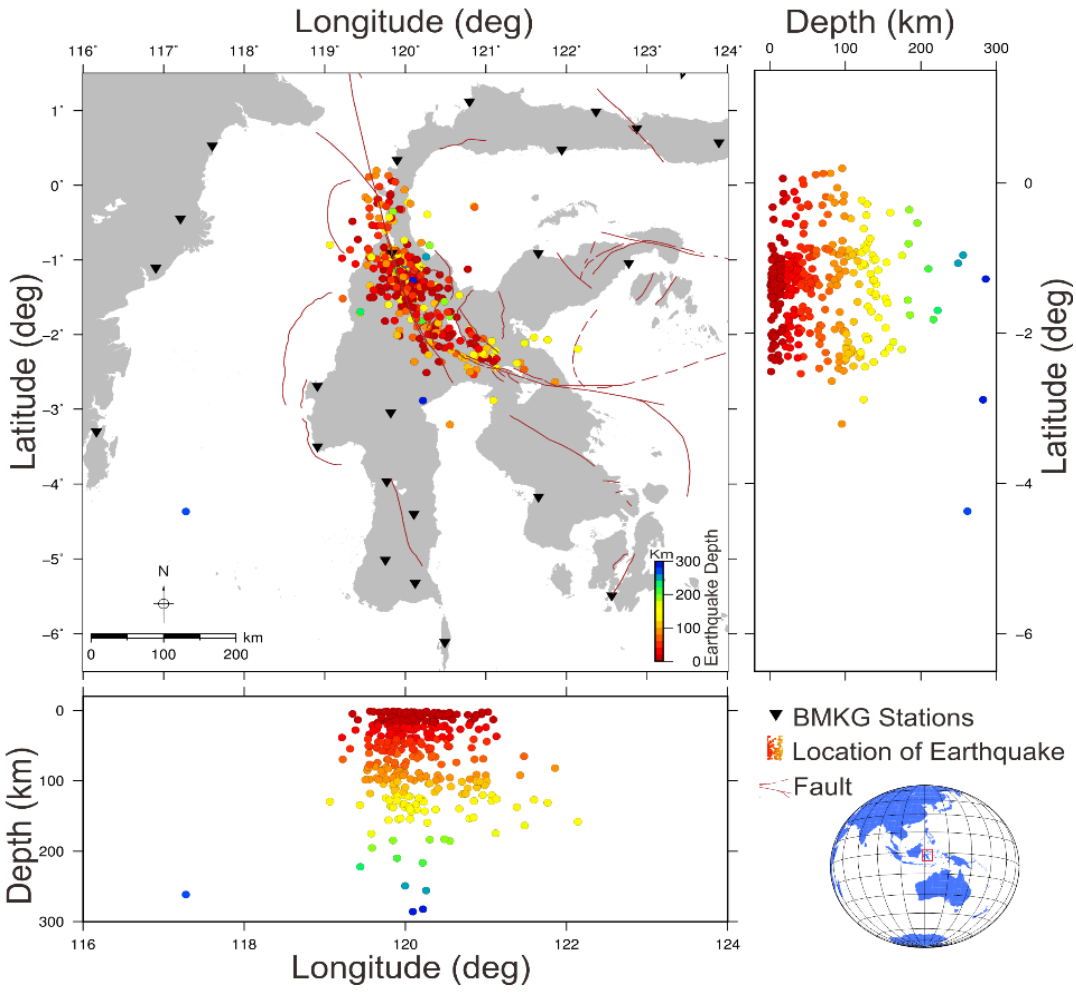

Figure 8. The horizontal and vertical distribution map of seismicity in the studied area. The red and blue dots indicate the locations of earthquakes according to the depths recorded by various observation stations, denoted by a black inverted triangle. The continuous red line depicts the position of geological formations represented as faults.

The NLLoc software demonstrated superior efficacy in identifying the hypocenter location (Figure 8). The events analyzed by the non-linearly distributed method demonstrate enhanced clustering in specific areas, due to the manual time-of-arrival retrieval process, stations distribution, a model of velocity, as well as the inversion method that was utilised in this research. This is further substantiated by the residual traveltime histogram (Figure 9). To monitor the residual travel time via a frequency distribution histogram to understand the discrepancy between observed and calculated journey time. This distribution pattern often exhibits a Gaussian distribution centered at zero, with increasing time differences, both positive and negative, correlating with more significant estimated inaccuracy. The outcomes from NLLoc exhibit more events with residual times approaching zero. The identical methodology utilized in a prior study conducted in Java [25], [26] likewise demonstrated substantial enhancement.

Unlike other methods (Geiger), which employ a linear framework in data inversion to ascertain the earthquake source's position (hypocenter), it linearly simplifies the link between parameters and observational data through iteration. The non-linear technique employs flexibility in the relationship among the processed variables, eliminating the necessity for linearization, which may result in systematic mistakes akin to those observed in the Geiger method.

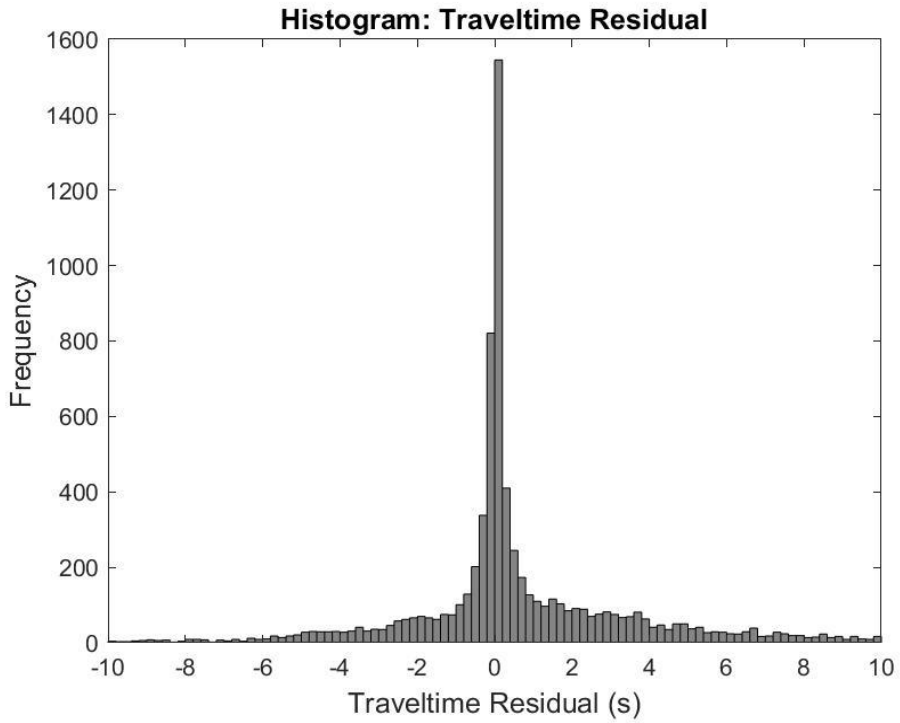

Figure 9. Histogram of the residual travel time from the estimation of the hypocentral distribution limited to the range of 10 to 10 seconds.

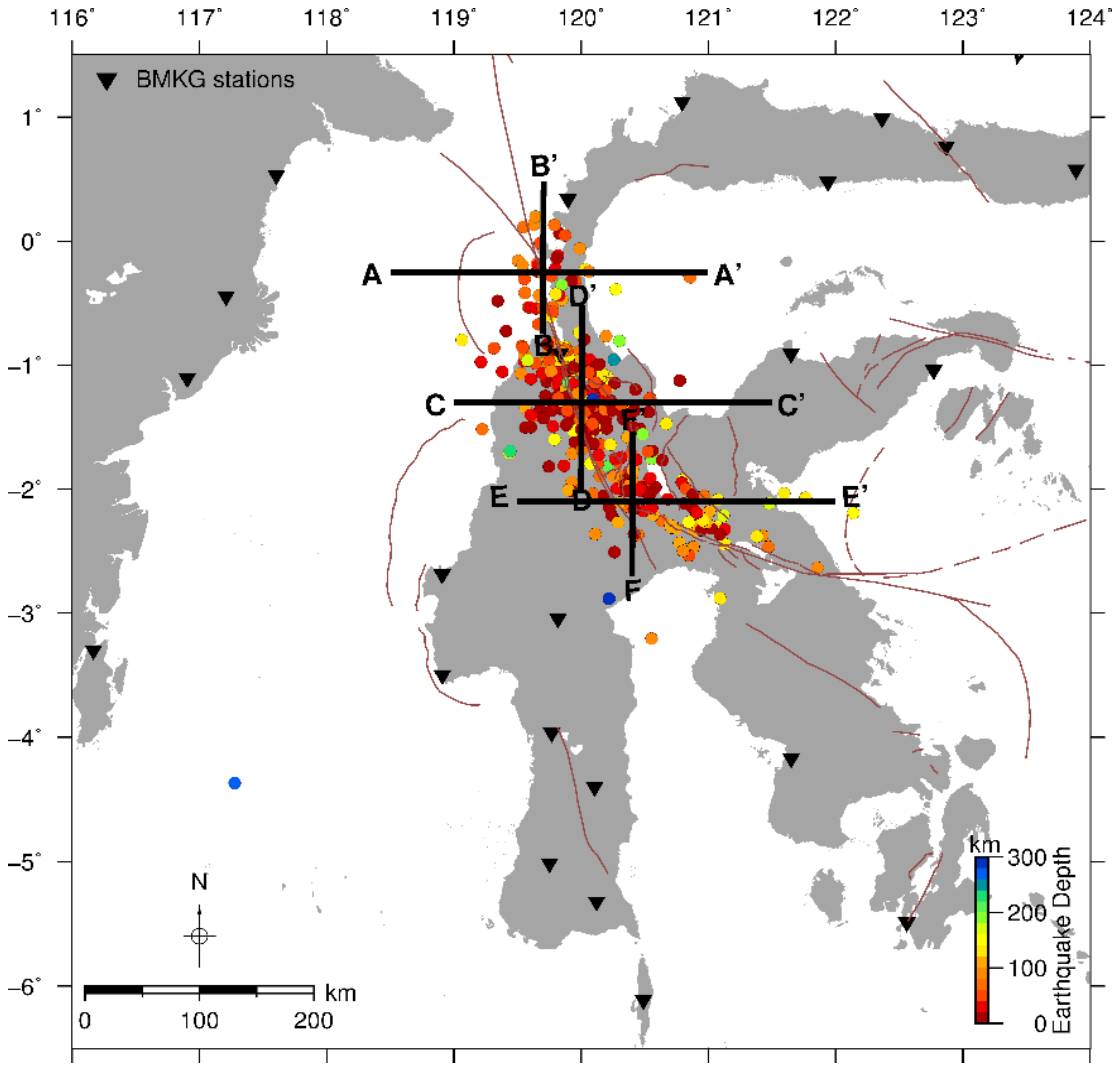

Figure 10. Our first findings indicate that the distribution of earthquake hypocentres in the vicinity of the active Palu-Koro fault aligns in a northwest-southeast orientation, reflecting the trajectory of the active Palu-Koro fault. The hypocenter locations cluster and align with the orientations of both the Palu-Koro and Matano faults. These findings align with prior research concerning the active Palu-Koro fault and its vicinity, utilizing alternative analyses and data from the BMKG catalogue.

Our first findings indicate that the distribution of earthquake hypocentres in the vicinity of the active Palu-Koro fault aligns in a northwest-southeast orientation (Figure 10), reflecting the trajectory of the active Palu-Koro fault. The hypocenter locations cluster and align with the orientations of both the Palu-Koro and Matano faults. These findings align with prior research concerning the active Palu-Koro fault and its vicinity, utilizing alternative analyses and data from the BMKG catalogue [19], [41].

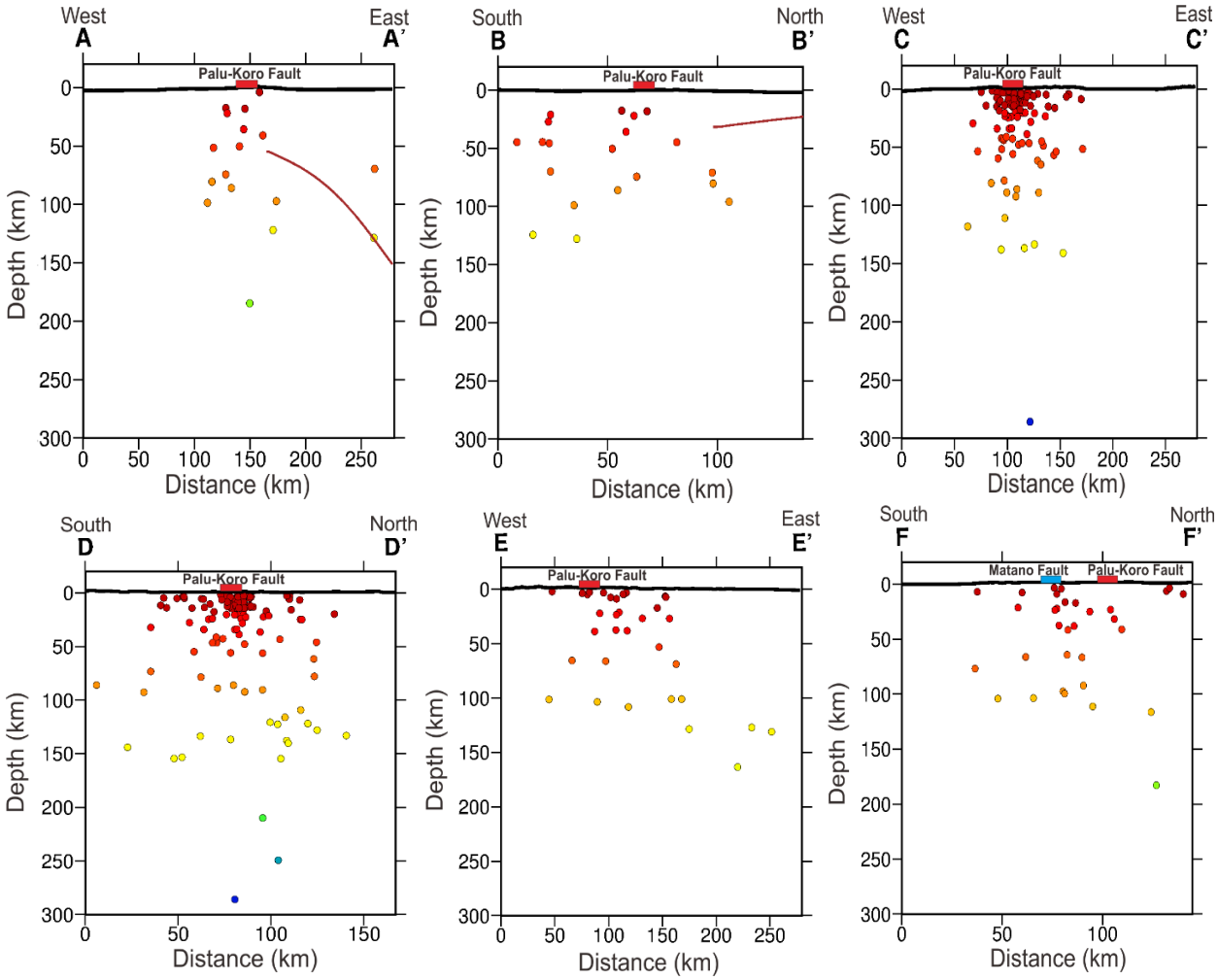

Figure 11. Cross-section results of the cross-section containing earthquake hypocentres in the Palu-Koro active fault area. The colored dots represent the hypocenter of the earthquake event.

Based on the location of the cross-section on the seismicity map, the results illustrate how the depth projection of the hypocenter, where the projection shows the subsurface model (Figure 11). In cross-section A-A', which is west-east trending and intersects the Palu-Koro fault line that is still active, the earthquake hypocentres are seen to gather on the Palu-Koro fault line that is still active with depths ranging from 1 - 200 km, following the path of the slab [42] given by the red colour line. Cross section B-B', which is south-north orientated and intersects the Palu-Koro active fault line, shows that the earthquake hypocentres are scattered along the Palu-Koro active fault line with depth variations from 1 - 120 km and have shallow to medium earthquake types. Meanwhile, the cross-section C-C', which is west-east trending and intersects the active fault line of Palu-Koro, shows excellent condition. This can be seen from the fact that most of the hypocentres are located just below the active fault line of Palu-Koro with a depth of 1 - 150 km and have shallow to medium earthquake types. The same thing also happens in a cross-section D-D' in the south-north direction. Although the hypocentres are scattered, there are visible gathering points of the hypocentres. The hypocentres we mean are the active fault lines of Palu-Koro with earthquake depths from shallow to deep. For cross

sections E-E‘ and F-F,’ the characteristics of the distribution of the hypocenter points are almost the same, i.e. the model is scattered, and there is a gathering point that illustrates the location of the active Palu-Koro fault line, except that for F-F' it is not very significant because in this path there is also the active Matano fault line which is located to the east of the active Palu-Koro fault.

Overall, seismic activity site in the vicinity of the Palu-Koro fault that is active is concentrated mainly on land. It is assumed that the main cause of the earthquake is the active Palu-Koro fault. Conversely, the research area is also affected by the surrounding faults, particularly the Palolo, Sausu and Matano faults. In addition, geological structural activities may occur at different times. This is demonstrated by the western Sulawesi Mandala, it is distinguished by the Mamuju fault, and the eastern Sulawesi Mandala is distinguished by the Poso fault and the Wekuli fault. Both of these faults are located in the same area.

The result of exact hypocenter position determination are significantly pertinent and applicable to catastrophe risk mitigation, both in the immediate term (e.g., early warning) and long term (e.g., spatial and infrastructural design). These findings serve as a crucial instrument in formulating disaster risk preventive and mitigation methods, thereby preserving numerous lives and minimizing the destruction inflicted by natural catastrophes.

Conclusion

We used a nonlinear technique to determine the hypocentral coordinates of 376 events in the active fault zone of Palu-Koro. The results of the NLLoc effort have significantly improved the localization of the events. The events analyzed by the nonlinear method show greater density in specific areas due to manual extraction of arrival times, distribution of stations, speed models, and inversion techniques used in this study. Specially concentrated areas may be affected by tectonic activity and active geological faults. The preliminary results will enable 1D speed modelling, event relocation, and 3D the seismic tomography of the active Palu Koro fault is for future studies focused on reducing earthquake disasters. This study's results enhance our comprehension of local seismic activity and reinforce the theoretical framework and methodologies employed in geophysical research for more precise determination of hypocenter locations. This work is anticipated to exert a lasting influence in both scientific research and practical applications for natural disaster risk mitigation. Consequently, it is imperative to utilize data with a broader and more concentrated distribution of recording stations in each location to minimize potential data bias by obtaining access to data from more earthquake recording organizations.

Acknowledgment

We thank the Meteorological, Climate and Geophysical Agency (BMKG) for providing earthquake data for the research, which can be found at https://geof.bmkg.go.id/webdc3/. In addition, we also thank Professor Anthony Lomax for creating the NNLoc and Seisgram2k70 programs for our data processing needs. All images used in this study were generated using Generic Mapping Tools software developed by Paul Wessel and Walter H.F. Smith.

References

[1] S. J. Hutchings and W. D. Mooney, "The Seismicity of Indonesia and Tectonic Implications," *Geochem Geophys Geosyst*, vol. 22, no. 9, p. e2021GC009812, Sep. 2021.

[2] M. Earle, "Protolith origin and plate tectonic setting of metamorphic complexes in the Timor fold and thrust belt, Indonesia," *Earth-Science Reviews*, vol. 246, p. 104589, Nov. 2023.

[3] R. Hall and M. E. J. Wilson, "Neogene sutures in eastern Indonesia," *Journal of Asian Earth Sciences*, vol. 18, no. 6, pp. 781–808, Dec. 2000.

[4] A. Guntoro, "The formation of the Makassar Strait and the separation between SE Kalimantan and SW Sulawesi," *Journal of Asian Earth Sciences*, vol. 17, no. 1–2, pp. 79–98, Feb. 1999.

[5] C. DeMets, R. G. Gordon, and D. F. Argus, "Geologically current plate motions," *Geophysical Journal International*, vol. 181, no. 1, pp. 1–80, Apr. 2010.

[6] R. E. Brackenridge, U. Nicholson, B. Sapiie, D. Stow, and D. R. Tappin, "Indonesian Throughflow as a preconditioning mechanism for submarine landslides in the Makassar Strait," *SP*, vol. 500, no. 1, pp. 195–217, Jan. 2020.

[7] G. Fang *et al.*, "Dynamic analysis of geophysical characteristics of Una-Una Volcanic Island, Sulawesi, Indonesia," *Journal of Asian Earth Sciences*, vol. 255, p. 105767, Oct. 2023.

[8] S. Supartoyo, C. Sulaiman, and D. Junaedi, "Kelas tektonik sesar Palu Koro, Sulawesi Tengah," *Jurnal Lingkungan dan Bencana Geologi*, vol. 5, no. 2, Art. no. 2, Aug. 2014.

[9] P. Bird, "An updated digital model of plate boundaries," *Geochem Geophys Geosyst*, vol. 4, no. 3, p. 2001GC000252, Mar. 2003.

[10] O. Bellier *et al.*, "High slip rate for a low seismicity along the Palu-Koro active fault in central Sulawesi (Indonesia)," *Terra Nova*, vol. 13, no. 6, pp. 463–470, Dec. 2001.

[11] G. Hui, S. Li, P. Wang, Y. Suo, Q. Wang, and I. D. Somerville, "Linkage between reactivation of the sinistral strike-slip faults and 28 September 2018 Mw7.5 Palu earthquake, Indonesia," *Science Bulletin*, vol. 63, no. 24, pp. 1635–1640, Dec. 2018.

[12] I. M. Watkinson and R. Hall, "Fault systems of the eastern Indonesian triple junction: evaluation of Quaternary activity and implications for seismic hazards," *Geological Society, London, Special Publications*, vol. 441, no. 1, pp. 71–120, 2017.

[13] A. Socquet *et al.*, "Microblock rotations and fault coupling in SE Asia triple junction (Sulawesi, Indonesia) from GPS and earthquake slip vector data," *J. Geophys. Res.*, vol. 111, no. B8, p. B08409, 2006.

[14] A. Walpersdorf, C. Vigny, P. Manurung, C. Subarya, and S. Sutisna, "Determining the Sula block kinematics in the triple junction area in Indonesia by GPS," *Geophys. J. Int.*, vol. 135, no. 2, pp. 351–361, Nov. 1998.

[15] G. Rachman *et al.*, "Seismic Structure Beneath the Molucca Sea Collision Zone from Travel Time Tomography Based on Local and Regional BMKG Networks," *Applied Sciences*, vol. 12, no. 20, p. 10520, Oct. 2022.

[16] Syamsidik, Benazir, M. Umar, G. Margaglio, and A. Fitrayansyah, "Post-tsunami survey of the 28 September 2018 tsunami near Palu Bay in Central Sulawesi, Indonesia: Impacts and challenges to coastal communities," *International Journal of Disaster Risk Reduction*, vol. 38, p. 101229, Aug. 2019.

[17] A. Y. Baeda, "Seismic and Tsunami Hazard Potential in Sulawesi Island, Indonesia," *Journal of International Development and Cooperation*, vol. 17, no. 1, pp. 17–30, 2011.

[18] P. S. Thein *et al.*, "Estimation of S-wave Velocity Structure for Sedimentary Layered Media Using Microtremor Array Measurements in Palu City, Indonesia," *Procedia Environmental Sciences*, vol. 28, pp. 595–605, 2015.

[19] H. Jayadi *et al.*, "A Preliminary Tomography Inversion Study on the Palu Koro Fault, Central Sulawesi Using BMKG Seismic Network," *IOP Conf. Ser.: Earth Environ. Sci.*, vol. 1227, no. 1, p. 012032, Aug. 2023.

[20] P. Supendi *et al.*, "Hypocenter relocation of the aftershocks of the Mw 7.5 Palu earthquake (September 28, 2018) and swarm earthquakes of Mamasa, Sulawesi, Indonesia, using the BMKG network data," *Geosci. Lett.*, vol. 6, no. 1, p. 18, Dec. 2019.

[21] N. Nurdin, D. Pujiastuti, and M. Marzuki, "Seismic deformation of the Palu Koro fault due to the 2018 Palu earthquake using global navigation satellite system data," *AIP Conference Proceedings*, vol. 2891, no. 1, p. 090014, May 2024.

[22] K. At-diena Putrie and S. Husein, "Imaging the Fault Plane Structure of Palu-Koro Fault from Earthquake Data Using Python," *IOP Conf. Ser.: Earth Environ. Sci.*, vol. 1373, no. 1, p. 012066, Jul. 2024.

[23] A. Lomax, J. Virieux, P. Volant, and C. Berge-Thierry, "Probabilistic Earthquake Location in 3D and Layered Models," in *Advances in Seismic Event Location*, vol. 18, C. H. Thurber and N. Rabinowitz, Eds., Dordrecht: Springer Netherlands, pp. 101–134, 2000.

[24] A. Abbasi, "Linear and nonlinear earthquake location approaches in a case study overview," *Physics of the Earth and Planetary Interiors*, vol. 293, p. 106265, Aug. 2019.

[25] S. Rosalia, S. Widiyantoro, A. Dian Nugraha, H. Ash Shiddiqi, P. Supendi, and Wandono, "Hypocenter Determination Using a Non-Linear Method for Events in West Java, Indonesia: A Preliminary Result," *IOP Conf. Ser.: Earth Environ. Sci.*, vol. 62, p. 012052, Apr. 2017.

[26] F. Muttaqy, A. Dian Nugraha, N. T. Puspito, P. Supendi, and S. Rosalia, "A Non-Linear Method for Hypocenter Determination around Central and East Java Region: Preliminary Result," *IOP Conf. Ser.: Earth Environ. Sci.*, vol. 318, no. 1, p. 012008, Aug. 2019.

[27] G. Rachman, B. J. Santosa, S. Rohadi, A. D. Nugraha, and S. Rosalia, "Preliminary Results: Probabilistic Non-Linear Method to Determine the Hypocenter Location in the Molucca Sea Collision Zone from BMKG Networks," *IOP Conf. Ser.: Earth Environ. Sci.*, vol. 873, no. 1, p. 012026, Oct. 2021.

[28] J. F. Di Leo *et al.*, "Deformation and mantle flow beneath the Sangihe subduction zone from seismic anisotropy," *Physics of the Earth and Planetary Interiors*, vol. 194–195, pp. 38–54, Mar. 2012.

[29] A. Patria and P. S. Putra, "Development of the Palu–Koro Fault in NW Palu Valley, Indonesia," *Geosci. Lett.*, vol. 7, no. 1, pp. 1–11, Dec. 2020.

[30] W. B. Hamilton, *Tectonics of the Indonesian region*, vol. 1078. US Government Printing Office, 1979.

[31] J. A. Katili, "Review of past and present geotectonic concepts of eastern indonesia," *Netherlands Journal of Sea Research*, vol. 24, no. 2–3, pp. 103–129, Nov. 1989.

[32] A. Jaya, O. Nishikawa, and S. Jumadil, "Distribution and morphology of the surface ruptures of the 2018 Donggala–Palu earthquake, Central Sulawesi, Indonesia," *Earth Planets Space*, vol. 71, no. 1, p. 144, Dec. 2019.

[33] O. Bellier, M. Sébrier, D. Seward, T. Beaudouin, M. Villeneuve, and E. Putranto, "Fission track and fault kinematics analyses for new insight into the Late Cenozoic tectonic regime changes in West-Central Sulawesi (Indonesia)," *Tectonophysics*, vol. 413, no. 3–4, pp. 201–220, Feb. 2006.

[34] S. Valkaniotis, A. Ganas, V. Tsironi, and A. Barberopoulou, "A preliminary report on the M7.5 Palu earthquake co-seismic ruptures and landslides using image correlation techniques on optical satellite data," *Report submitted to EMSC*, pp. 1–15, 2018.

[35] T. J. Moser, T. Van Eck, and G. Nolet, "Hypocenter determination in strongly heterogeneous Earth models using the shortest path method," *J. Geophys. Res.*, vol. 97, no. B5, pp. 6563–6572, May 1992.

[36] A. Tarantola and B. Valette, "Inverse problems = Quest for information," *J Geophys*, vol. 50, no. 1, pp. 159–170, Oct. 1981.

[37] A. Lomax and A. Curtis, "Fast, probabilistic earthquake location in 3D models using oct-tree importance sampling," in *Geophys. Res. Abstr*, pp. 10–1007, 2001.

[38] J. Havskov and L. Ottemoller, "Routine Data Processing in Earthquake Seismology : With Sample Data Exercises and Software", Springer, 2010.

[39] S. Husen, "Probabilistic Earthquake Relocation in Three-Dimensional Velocity Models for the Yellowstone National Park Region, Wyoming," *Bulletin of the Seismological Society of America*, vol. 94, no. 3, pp. 880–896, Jun. 2004.

[40] A. L. G. Pinho, "Probabilistic non-linear earthquake location in a 3–D velocity model," 2008.

[41] M. Muhammad Fawzy Ismullah, A. Dian Nugraha, M. Ramdhan, and Wandono, "Precise Hypocenter Determination around Palu Koro Fault: a Preliminary Results," *IOP Conf. Ser.: Earth Environ. Sci.*, vol. 62, p. 012056, Apr. 2017.

[42] G. P. Hayes *et al.*, "Slab2, a comprehensive subduction zone geometry model," *Science*, vol. 362, no. 6410, pp. 58–61, Oct. 2018.